6.1 Introduction

Wollastonite is a calcium silicate mineral with the chemical formula $CaSiO_3$. According to its crystal structure, it is among the pyroxenoid group of inorganic materials containing infinite chains of [SiO_4] tetrahedral (Deer *et al*., 1997). The chain motif in wollastonite is formed by two apex-to-apex combination tetrahedra, one of which is a tetrahedron with a corner parallel to the Si-O chain direction. The Si-O chains are co-ordinated to Ca (Ohashi, 1984). It has a polymorphic structure, the most common triclinic or monoclinic phase is a low-temperature phase, i.e., β-$CaSiO_3$ (para wollastonite), and the other is a high-temperature phase, i.e., α-$CaSiO_3$ (pseudo wollastonite) (Florian *et al*., 2009). Some properties, i.e., its low dielectric constant, low dielectric loss, low volatile content, high brightness, whiteness, low shrinkage, low thermal expansion, low moisture absorption, thermal stability and fluxing properties, of wollastonite are highly useful for industrial applications (Sen, 1992). The application of wollastonite by the ceramic industries to obtain ceramics with better performance parameters is increased rapidly. Sales are also improved worldwide by 30% to 40%. It also offers useful applications for other industries, such as applications as a metallurgical flux for welding, as an additive in paints, as plastics to improve tensile and flexural strength, as a material for civil construction, and as a medical material for artificial bones and dental roots (Virta, 2009; Liu *et al*., 2004). World demand for wollastonite is therefore steadily expanding.

Many researchers consequently studied ways of fabricating synthetic wollastonite for different purposes using various raw materials and synthesis techniques. Vakalova *et al*. (2016) have derived wollastonite through mixtures of calcium carbonate with technogenic siliceous stock (micro silica, gaize or diatomite) by a solid-state method. Papynov *et al*. (2017) have synthesized porous wollastonite ceramic using a combination of sol-gel (template) and spark plasma-sintering (SPS) processes. Leite *et al*. (2017) have produced wollastonite base insulating materials using avian eggshell waste as a source of calcium oxide (CaO) and chamotte as a source of silica (SiO_2). Vichaphund *et al*. (2011) have produced

wollastonite using eggshell waste through microwave synthesis. Ismail *et al.* (2016) have derived wollastonite from rice straw ash and limestone. Wu *et al*. (2012) have fabricated porous β-$CaSiO_3$ scaffolds for application in bone regeneration by a chemical precipitation method.

The present work is conducted to fabricate synthetic wollastonite using 100% abandoned ingredients, i.e., bio-waste eggshell and abandoned RHA by a conventional solid-state route. Special attention is given to the preparation characteristics of the synthesized wollastonite and the dielectric properties of the sintered β and α-wollastonite.

6.2 Experimental Procedure

Wollastonite powder was synthesized using a stoichiometric (1:1 molar) amount of calcined eggshells (~99% CaO) and heat-treated RHA (~93% SiO_2) as ingredients. The wollastonite powder preparation process was described in the chapter 3. For the pellet formation, the calcined grinding powder was granulated with 3 wt.% polyvinyl alcohol (PVA) as a binder and pressed under a uniaxial hydraulic press at a pressure of 200 MPa. The pressed plates were than sintered at the calcination temperatures (to maintain the phases well), i.e., 1100°C calcined powder was sintered at 1100°C and 1200°C calcined powder was sintered at 1200°C in an air atmosphere with a heating and cooling rate 2ºC/min and a soaking period of 4 h.

6.3 Results and discussion

6.3.1 Characterization of calcined wollastonite

Powder XRD studies were performed at room temperature for calcined wollastonite powders after milling. Figure 6.1 shows the XRD patterns of calcined powders heated at 1000, 1100, 1150 and 1200°C. The formations of perovskite structures of β and α-wollastonite at different calcining temperatures have been confirmed. It can be seen that the peaks of β-wollastonite, small quantity larnite (Ca_2SiO_4) and unreacted cristobalite (SiO_2) are observed at 1000°C, matching those of JCPDS file numbers 43-1460, 33-0302 and 82-0512, respectively, and that the peaks of CaO are disappeared (Florian *et al*., 2009). The formation

of the pure wollastonite phase at low temperature was greatly affected by the finesse of the ingredients (Yazdani *et al*., 2013). It may be that highly active amorphous RHA silica and fine raw materials accelerate the diffusion reaction for the phase formation of wollastonite. Single-phase β-wollastonite (monoclinic, space group number and name-14, P21/a) is attained after calcination at 1100°C; and larnite and cristobalite are eliminated through reaction with each other. Additionally, the β-wollastonite, i.e., para wollastonite, phase is transformed to its polymorphic form of α-wollastonite, i.e. pseudo wollastonite, at high temperature (Nour *et al*., 2008). At 1150°C calcined powder is composed of collaborative α and β-wollastonite phases, and at 1200°C the powder comprises mainly the pseudo wollastonite phase (anorthic, C-1) (Florian *et al*., 2009; Vichaphund *et al*., 2011). The crystallite sizes of the β and α-wollastonite are projected from the X-ray peak broadening of the (320) and (132) peaks of 1100 and 1200°C calcined powders, respectively. The crystallite sizes increase with the transformation of β to α-wollastonite, to 62 and 83 nm, respectively. This effect occurs due to the formation of the pseudo-hexagonal structure of α-$CaSiO_3$, which contains three silicon-oxygen tetrahedra and forms a ring of $Ca_3Si_3O_9$ (Xia *et al*., 2008).

In order to study the purity and formation of the chemical bonds during calcination at 1100 and 1200°C, FTIR analysis (shown in Figure 6.2) is performed. The formation of crystalline $CaSiO_3$ is recognized by the FTIR peaks at 432, 622 and 985 cm^{-1} (Beaudoin *et al*., 2008). A group of absorption bands in the region of 1000-1200 cm^{-1} represents asymmetric stretching vibration oscillations of the bridge bonds Si-O-Si in the [SiO_4]-tetrahedra. Strong absorption bands in the region of the spectrum at about 980 - 650 cm^{-1} is attributed to symmetrical stretching vibrations of the bridge and non-bridge Si-O bands (Shamsudin *et al*., 2017; Eniu *et al*., 2015). The bonds between the 600-450 cm^{-1} spectra are assigned to the bending vibrations of the bridge and non-bridge Si-O groups, (Paluszkiewicz *et al*., 2008) and the existence of Ca-O bonds in the structure, i.e., [CaO_6]-octahedra is confirmed by the peaks at 423-450 cm^{-1} and 940 cm^{-1} (Sharafabadi *et al*., 2017). The broad band at around 890 cm^{-1} is

assigned to the characteristic peaks of Si-O-Ca (Puntharod *et al*., 2013). These peaks verify the formation of wollastonite, as they are also shown in the XRD patterns of the powder, calcined at 1100°C and above.

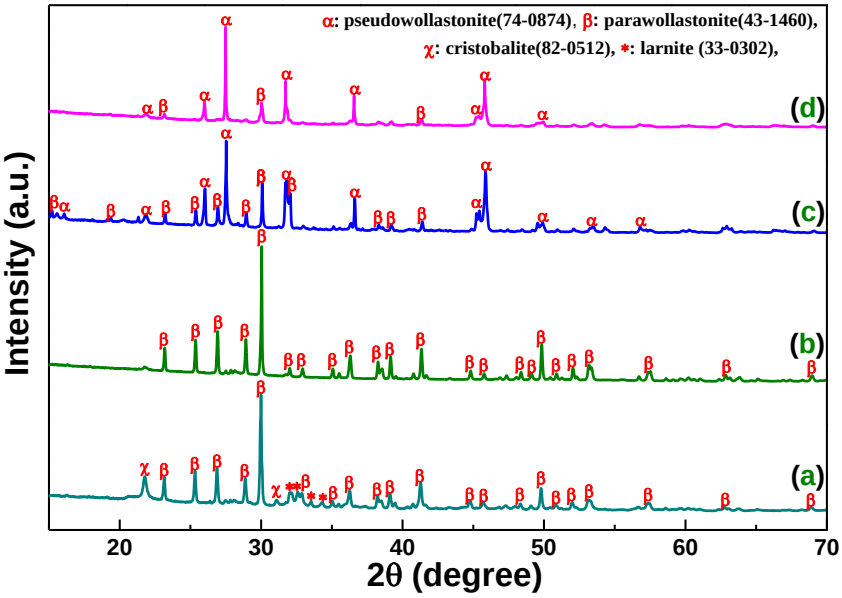

Figure 6.1 XRD analysis of calcined powders at (a) 1000, (b) 1100, (c) 1150 and (d) 1200°C.

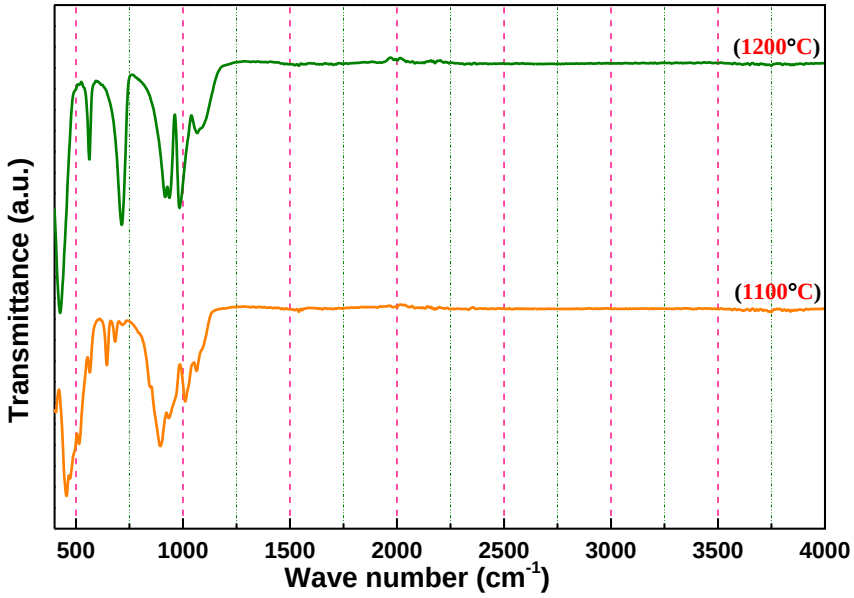

Figure 6.2 FTIR spectroscopy of wollastonite powders calcined at 1100 and 1200°C.

Figure 6.3 shows SEM micrographs and EDX analysis of powder calcined at 1100 and 1200°C for 2 h without grinding. The SEM results indicate that both powders are composed mainly of irregular agglomerate-shaped particles. There is a slight difference in the sizes of the wollastonite powders calcined at 1100 and 1200°C. It can be clearly observed that the

average particle size is improved with increases in the calcined temperature due to the stacking together of fine wollastonite particles at high temperature to form agglomerates (Leite *et al*., 2017). The average particle sizes are 2.10 and 3.60 μm for calcination at 1100 and 1200°C, respectively. It is also seen in the morphology that the texture of the particles becomes rougher with increase in the calcination temperature. EDX analysis of the calcined powder reveals that the quantitative existence of Ca, Si and O elements in approximately with their respective proportions, suggests high purity of the wollastonite powder.

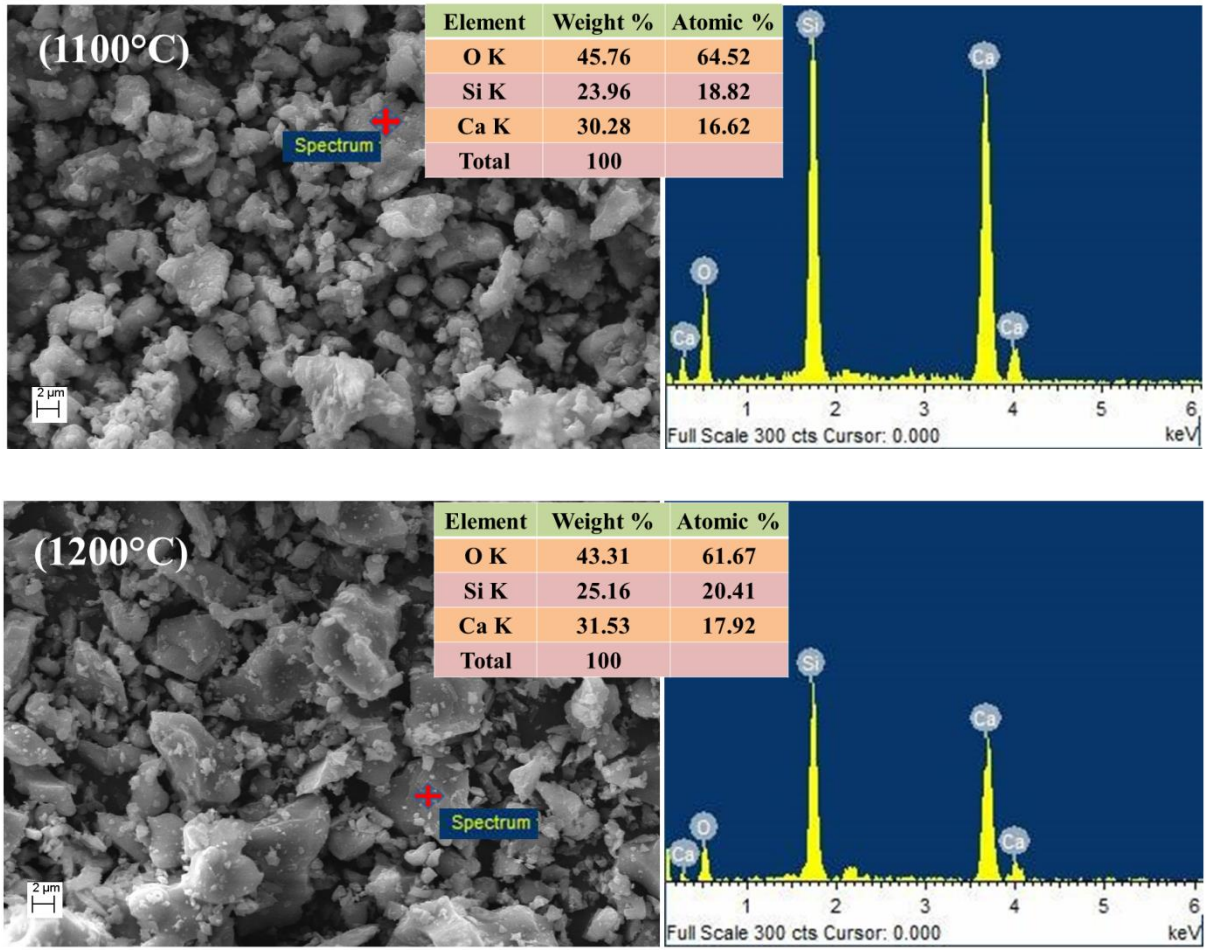

Figure 6.3 SEM and EDX analysis of wollastonite powders calcined at 1100 and 1200°C.

6.3.2 Characterization of sintered wollastonite

Figure 6.4 demonstrates the thermal densification curve of the waste-derived wollastonite powder, which is already calcined at 1200°C. No significant expansion or shrinkage behavior is observed up to 900°C. The graph shows that the compacted powders begin to densify at around 920°C and the rate of the shrinkage increases with the increase in

temperature. Closely similar sintering behavior is observed for wollastonite in the previous studies also (Karamanov and Pelino, 2008; Cannillo *et al*., 2009). The linear shrinkage values of wollastonite are 0.82, 3.9 and 6.27% for 1100, 1200 and 1250°C, respectively. These increases in the shrinkage values may be attributed to the densification of the powder.

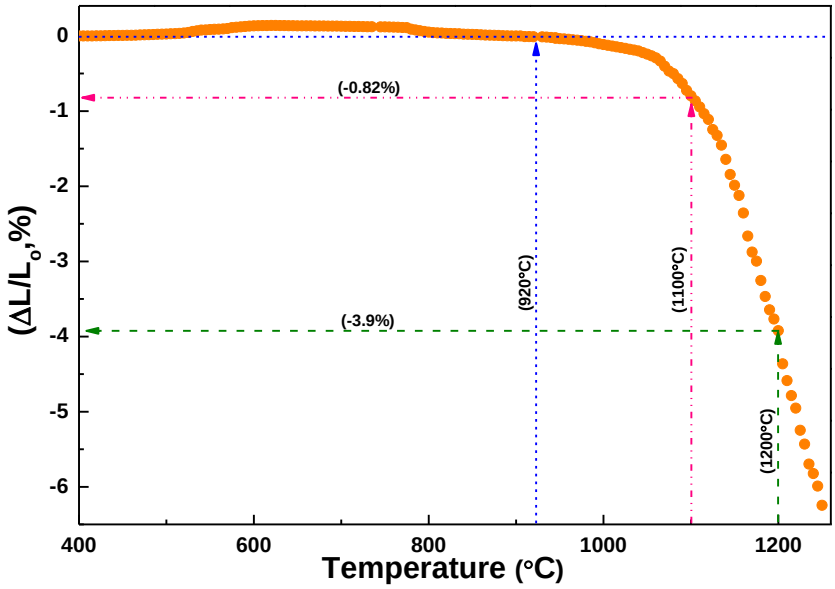

Figure 6.4 Shrinkage curve of 1200°C calcined wollastonite powder in air up to 1250°C.

SEM micrographs of the wollastonite surfaces sintered at 1100 and 1200°C are presented in Figure 6.5. The sintered specimen at 1100°C exhibits an interconnected porous structure. A large number of open pores with different shapes are detected. The grains are uneven in shape with sizes from 0.236 to 0.487 μm. An increase in the sintering temperature to 1200°C results in a dense structure with diffusion of the small grains, which enhances the size of the isometric grains of the crystalline phase and decreases the pore sizes. Vichaphund *et al*. (2011) have reported the same characteristics for sintered wollastonite. The values of apparent porosity, bulk density, average grain size and bending strength (BS) are shown in Table 6.1. The porosity shrinks, i.e., 23.37 % to 4.65% with increase in the sintering temperature. A second reason may be the formation of α-$CaSiO_3$ crystalline phases with a pseudo-hexagonal structure in the system. Si-O tetrahedra in the pseudo-wollastonite are therefore compacted further by the form of the ring structure. As a result, the surface energy

of the ring is increased. It may be reduced by introducing a large number of atoms to increase the volume of the ring and forms a compact structure by reorientation of the atoms (Tangboriboon *et al*., 2011).

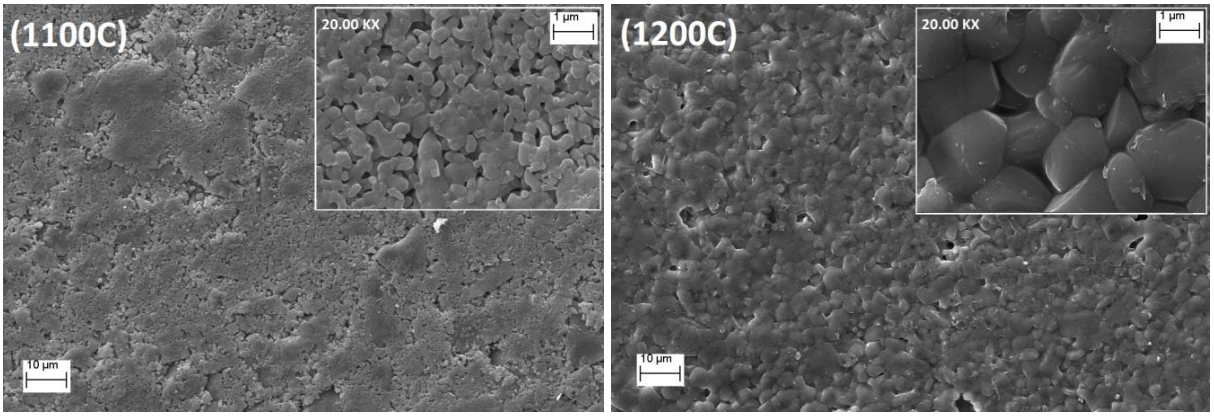

Figure 6.5 SEM micrograph of wollastonite sintered at 1100 and 1200°C.

Table 6.1 Apparent porosity, bulk density, grain size and flexural strength of sintered wollastonite samples.

Samples	Apparent porosity (%)		Bulk density (gm/cc)		Grain size (µm)		Bending strength (MPa)	
	Mean	s.d.	Mean	s.d.	Mean	s.d.	Mean	s.d.
1100°C	22.37	1.18	2.065	0.081	0.378	0.027	26.42	2.72
1200°C	4.65	0.87	2.603	0.046	1.235	0.013	68.85	1.63

The mean values for BS at room temperature of sintered wollastonite specimens are given in Table 6.1. The BS is significantly improved with increase in the densification temperature. This may be attributed due to the decrease in the porosity and the increase in the degree of sintering, as shown in the SEM micrograph and densification curve (Figure 6.4 and 6.5). Porosity in the non-ductile body accelerates the rate of crack propagation (Kazmi *et al*., 2016).

The room temperature frequency dependency of the dielectric constant (ε′), loss angle tangent (tanδ) and AC resistivity (ρ) of the wollastonite sintered at 1100 and 1200°C are measured in the frequency range of 20 Hz to 10 MHz, as displayed in Figures 6.6(a-c), respectively. The values of the above-mentioned electrical properties at 100 kHz are tabulated in Table 6.2. Both samples, i.e., 1100 and 1200°C sintered wollastonite, exhibit a low and stable dielectric constant up to a frequency of 1 MHz. This may be due to the low dielectric

polarizability of Si and Ca, which are strongly bonded in the [SiO_4]-tetrahedral and [CaO_6]-octahedra structural units of the $CaSiO_3$, resulting in polarization dominated by the hopping mechanism. Wollastonite exhibits a slight enhancement in the dielectric constant with increase in the sintering temperature from 1100 to 1200°C. This may be due to increase in the density of the sample with a lower porosity and uniform microstructure (Hu *et al*., 2015). Another reason may be the oxygen vacancy, which increases due to the increase in the space charge polarization, resulting increase dielectric constant. The tangent of loss (tanδ) is represented the portion of the electric energy which are dissipated to heat in the ceramic body by various physical relaxation processes. It can be observed in Figure 6.6(b) that tanδ is very low for both the samples. It is also seen that the dielectric loss is nearly independent of frequency up to 1 MHz. For this reasons, wollastonite is called a 'low loss ceramic' (Sen, 1992). This low tanδ can be attributed to the high electrical resistivity of ~10^{10} Ω-cm at 1 kHz. A slight decrease in ρ with increase in frequency is observed in Figure 6.6(c), moreover, due to the inverse relationship between them. It is important to maintain low-stable ε′ and tanδ in a relatively wide frequency range for the practical use of wollastonite as an ingredient in electrical porcelain bodies.

The changes in the dielectric constant and loss as a function of temperature for sintered samples at 1 MHz are presented in Figure 6.7(a, b), respectively. It is clear from Figure 6.7 that ε′ and tanδ are approximately constant from 30 to 480°C at 1 MHz for both the samples. These results suggest that the temperature does not alter the dielectric polarization mechanisms of wollastonite up to 480°C. It may be due to the presence of strong ionic bonds in the $CaSiO_3$.

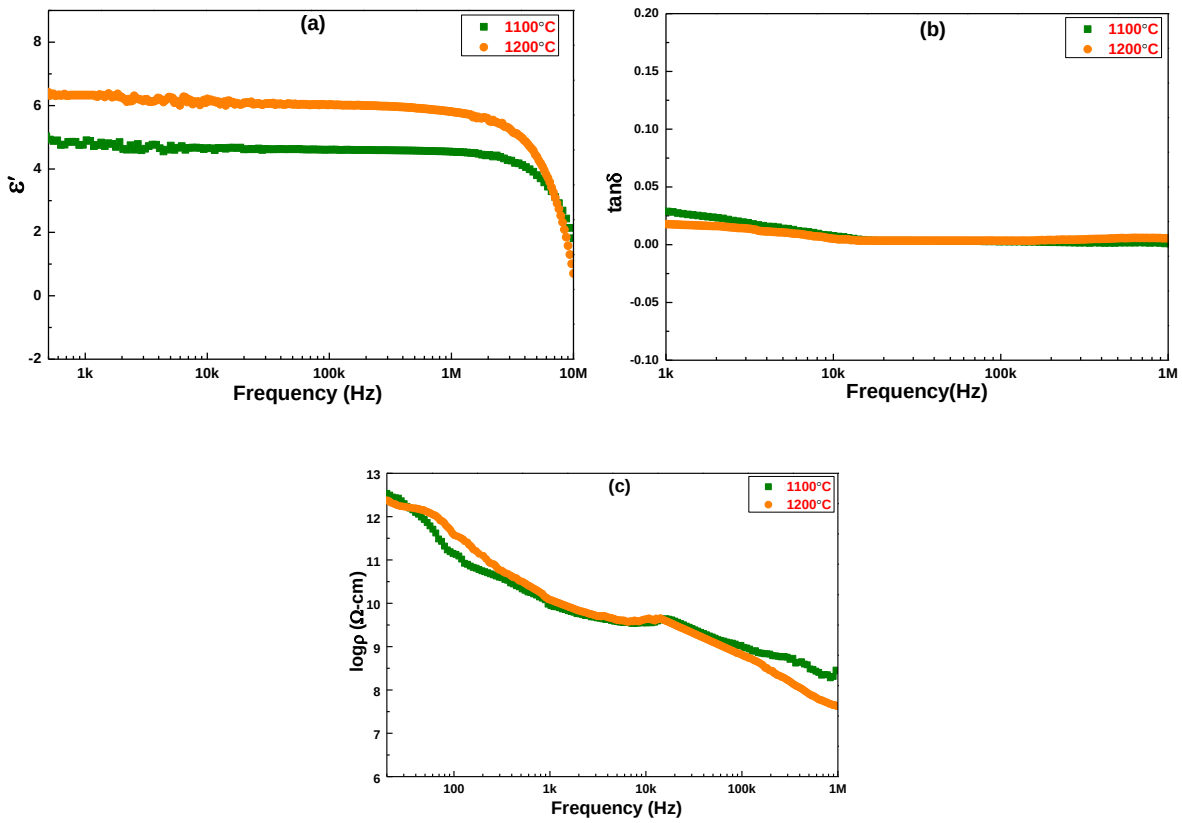

Figure 6.6 Change of (a) dielectric constant, (b) loss angle tangent (tanδ) and (c) electrical resistivity with frequency for samples sintered at 1100 and 1200°C.

Table 6.2 Dielectric constant, tangent of loss and resistivity of sintered samples.

Samples	Dielectric constant $(\varepsilon')_{100kHz}$	Loss angle tangent $(\tan\delta)_{100kHz}$	Resistivity $(\rho)_{100kHz}$ (Ω-cm)
1100°C	4.62	0.00260	9.60×10^{8}
1200°C	6.02	0.00361	6.42×10^{8}

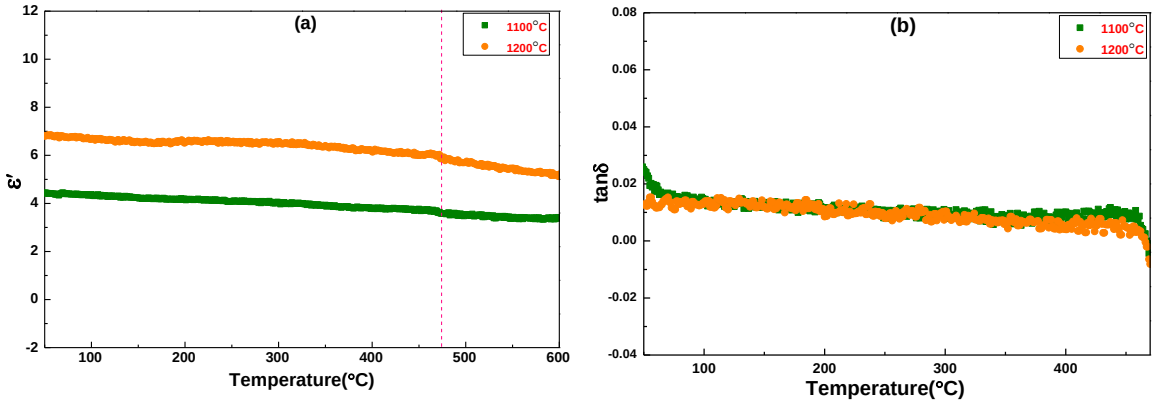

Figure 6.7 Change of (a) dielectric constant and (b) loss angle tangent (tanδ) with temperature for samples sintered at 1100 and 1200°C.

6.4 Summary

The results of this study demonstrate that chicken eggshells and RHA can be used for the production of sustainable, high-purity synthetic wollastonite as an ingredient for ceramics and other industrial products. The physical and dielectric properties of wollastonite are investigated. It is found that the peak of β-wollastonite, a small quantity of larnite (Ca_2SiO_4) and unreacted cristobalite (SiO_2) are detected at 1000°C and that only β-wollastonite is observed after calcination at 1100°C. Powder calcined at 1150 and 1200°C contains mainly α-wollastonite and a slight portion of unconverted β-wollastonite. The average particle and grain sizes increase with the increase in the calcined and densification temperatures of the wollastonite. The density and mechanical strength are also improved with the increase in the sintering temperature. The dielectric properties of wollastonite are not affected significantly by the transformation of β to α phase. The wide range of temperature (30 to 480°C) does not alter the dielectric behavior of the wollastonite. This recycling of wastes for wollastonite formation can lead to economical and sustainable ceramics production by putting it to a practical use in the electrical porcelain industry.